Correlation effects in x-ray spectra of Ni and Ni in Ni_3Mo

K. Ławniczak-Jabłońska
Institute of Physics, Polish Academy of Sciences, Aleja Lotnikow 32/46, PL-02 668 Warsaw, Poland

J. Inoue and T. Tohyama
Department of Applied Physics, School of Engineering, Nagoya University, Chikusa-ka, Nagoya 464-01, Japan

M. T. Czyżyk
Research Institute of Materials, University of Nijmegen, Toernooiveld, 6525 ED Nijmegen, The Netherlands
(Received 19 August 1993; revised manuscript received 13 December 1993)

An estimation of factors which can cause significant many-body effects in x-ray spectra of a given material is very important for understanding the physics behind these effects. In the present study this problem has been approached using the example of the x-ray emission spectra of elemental Ni and Ni in Ni_3Mo. The spectra were calculated within the one-electron model on the basis of partial density of states obtained by various methods, namely the tight-binding method, the linear-muffin-tin-orbital method, and the method of local spherical waves. The coherent-potential-approximation method suitable for random materials was additionally considered for Ni_3Mo. In the case of elemental Ni, the one-electron model fails and all applied methods result in an emission spectrum about 1.2 eV broader than the experimental spectrum. This discrepancy is not dependent on the method of calculation. For Ni_3Mo, all the considered methods provide the correct basic shape of the L_α spectrum, and calculated spectra differ only in details of the intensity distribution. The addition of a second element (Mo) leads to the increase of the Ni-Ni distance that results in reduction of the many-body effects. The observed broadening of the Ni spectra from Ni_3Mo as compared with the spectrum of elemental Ni is due to the decrease of the correlation effects.

I. INTRODUCTION

X-ray emission spectroscopy (XES) is the oldest method used for studying the electronic structure of metals and alloys.[1] A particular advantage of XES is that, in the case of alloys and compounds, this technique projects the local density of states (LDOS) at the site of an emitting atom. Furthermore, the XES method is especially suitable for studying the electronic structure of bulk materials because of the deep penetration of the x-ray signal in contrast with photoelectron spectroscopy. The disadvantage of XES is that the emission takes place in the presence of a hole in the inner shell; in the final state the hole in the outer shell is left. The convolution of the natural width of the inner shell with the density of states (DOS) smooths the fine structure. In many cases the presence of a hole does not practically influence additionally the distribution of valence DOS.

Generally, the one-electron model successfully describes the x-ray emission spectra for many materials. However, in some particular cases, when many-body effects take on an important role, this model fails. A well-known example is the case of the emission spectra of nickel.[2,3] This was also observed and widely discussed in literature for Ni photoelectron spectra.[4] The photoelectron emission happens in the absence of an inner-shell hole. Therefore the presence of the inner-shell hole is not combined with this effect. In both spectra the final state has a hole in the valence band. It indicates that interactions between this hole and a valence electron is responsible for narrowing the recorded Ni spectra. The question arises as to what can change the importance of many-body interactions in a given material. In the present study the x-ray emission spectra of Ni from Ni_3Mo were analyzed to address this question.

The binary Ni-Mo system belongs to the class of alloys with a limited solid solubility.[5] Up to 25% of Ni atoms can be substituted with Mo atoms in the fcc lattice of nickel. For higher Mo content, a phase transition takes place or a phase mixture appears. In the Mo concentration range from 20 to 70 at. % an amorphous phase can be easily formed.[6] Furthermore, the Mo/Ni multilayered samples exhibit very promising properties.[7] NiMo has also been formed by mechanical alloying.[8] At the limit of solid solubility Ni_3Mo can be crystallized by special heat treatment in the random face-centered-cubic (fcc) structure or in a long-range-ordered orthorhombic structure (ort.). The melting point of the Ni-Mo system is close to 1700 K (1588 K for Ni_3Mo). This resulted in wide application of Ni-Mo alloys in the production and protection of industrial tools. The alloys discussed are thus a very stimulating model material for studying the atomic processes, and very interesting from the point of view of commercial applications.

The description of crystal structure in alloys is complex, and depends on the degree of ordering. The statistical ordering, which is visible in x-ray diffraction experiments, can differ from the local ordering.[9,10] To calculate the electronic structure, one should assume the model of structure and occupancy in atomic positions.

Nowadays a number of methods is available for computing the electronic structure. The methods applied in this paper differ in the form of the Hamiltonian used and the accuracy of the computation. We chose fluorescence spectroscopy as a method with sufficient reliability to check the calculations.

XES is a unique method enabling the testing of the partial density of states for each component separately, and can provide information about the full valence-band width. In this paper we address the problem of the occupied states. A discussion of the structure of unoccupied valence states together with relevant experimental results [x-ray-absorption spectroscopy (XAS) and bremsstrahlung isochromat spectroscopy (BIS)] has already been presented elsewhere.[11] The correlation effects appear unimportant for K absorption, and isochromat spectra for elemental Ni and for the Ni_3Mo alloy.

The experimental details of measurements of the fluorescence Ni spectra are given in Sec. II. Several theoretical methods used to calculate the local partial DOS and total DOS for elemental Ni and Ni in the alloy considered are briefly presented in Sec. III. The DOS obtained by different methods were the basis for calculations of the Ni x-ray L_α emission spectra within the one-electron model. A comparison of the calculated and measured spectra for elemental Ni and Ni in Ni_3Mo alloys is reported in Sec. IV. This comparison enables us to identify the influence of correlation effects on the shape of Ni-emission spectra. We discuss also the importance of the two-vacancy satellite and self-absorption. Finally, in Sec. V a short summary is presented.

II. EXPERIMENT

The polycrystalline Ni_3Mo samples were prepared from high purity Goodfellow metals by repeated arc melting of a weighed amount of materials in a helium atmosphere. An x-ray microprobe was used to check the chemical composition at several different regions of the samples. The samples were found to be homogeneous. The ingots were cut into 0.5–1.0-mm thick slices. The crystal structure of the Ni_3Mo samples were formed by special thermal treatment. The fcc random structure was created by annealing for one week in a vacuum of 10^{-6} Pa at a temperature of 1273 K, and then quenching to room temperature. To establish the orthorhombic long-range-ordered structure, the samples were annealed for four days at a temperature of 1013 K.

The structures were determined by x-ray diffraction. No traces of foreign phases were detected in the random samples. The fcc lattice parameter was estimated to be equal to 3.630(4) Å. The parameters of the orthorhombic structure of the ordered sample were found to be equal to $a=5.066(6)$ Å, $b=4.227(3)$ Å, and $c=4.457(4)$ Å. Within the limits of error, these values correspond to data presented in the literature.[5] Small traces of tetragonal phases were detected in this sample. The long-range-order coefficient was estimated to be better than 0.88.

A single-crystal fluorescence spectrometer equipped with a RAP ($C_8H_5O_4R_6$) crystal was used to measure the Ni L_α emission spectra. The energy resolution of the recorded spectra was equal to 0.5 eV. The radiation source used to excite the L_α spectra was a copper anode x-ray tube operating at 8 kV and 195 mA.[3] A gas flow proportional counter was used as a detector. The spectra were recorded at 0.1-eV steps. The time chosen for measurement was identical at each step, and provided at least 2000 counts at maximum, after linear subtraction of the background. The statistical error of counts was slightly larger than the size of the point marked in the figures. The spectra for each sample were recorded repeatedly at least three times, and were found to be well reproducible. A linear background was subtracted from each spectrum. No further data corrections were performed.

III. ELECTRON BAND-STRUCTURE CALCULATIONS

A. Tight-binding approximation

The tight-binding d-band model was used to calculate the d-DOS for Ni. This model was adopted to calculate the d-LDOS and total density of states (TDOS) for alloys under the assumption of the $L1_2$ and orthorhombic types of unit cells.[12,13] Annealing the random Ni_3Mo alloy at a temperature below 740 °C results in the appearance of an orthorhombic close-packed structure (ort.) which belongs to the space group $Pmmn$ (D_{2h}^{13}).[5,14] The unit cell contains eight atoms in the following Wyckoff positions:

Mo $2a$ $(0,0,z_a)$ with $z_a=\frac{1}{2}+z_c$,

Ni $2b$ $(0,1/2,z_b)$ with $z_b=1-z_a$,

Ni $2f$ $(x,0,z_c)$ with $z_c=0.0157$ and $x=\frac{1}{4}$.

These data were the relevant input parameters for tight-binding d-band calculations. The values of parameters $dd\sigma$, $dd\pi$, and $dd\delta$ (Ref. 12) were calculated using the Pettifor formula.[15] The Wigner-Seitz sphere radius and

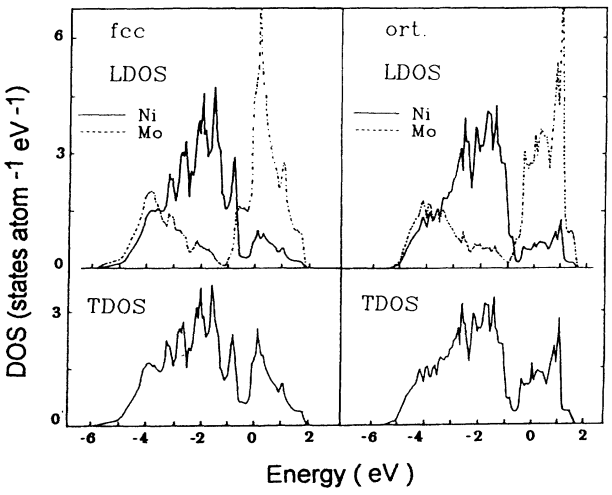

FIG. 1. The d-LDOS and TDOS calculated by making use of the tight-binding d-band model for $L1_2$ and orthorhombic structures of the Ni_3Mo alloy.

the effective mass were taken from Andersen and Jepsen.[16] The TDOS and LDOS were calculated using the tetrahedron method.[17] Values of the atomic potentials were determined self-consistently to satisfy the charge-neutrality condition at each atomic site. The charge-neutrality condition for the Mo-Ni system was confirmed experimentally by the x-ray emission study[3] and the x-ray photoelectron study.[18] As a result of the charge neutrality, the high-energy part of the DOS (antibonding orbitals) is due mainly to the Mo d bands, and the low-energy part (bonding orbitals) is due to the Ni d bonds (Fig. 1).

B. Localized spherical-wave method

The electron band-structure calculations for Ni and for the Ni_3Mo alloy, assuming $L1_2$ and orthorhombic structures, were also performed using the localized spherical-wave (LSW) method.[19]

The scalar-relativistic Hamiltonian (spin-orbit interaction not included) with exchange and correlation effects treated within the local- (spin-) density approximation using the (spin-polarized) Hedin-Lundqvist parametrization was assumed in this method. Self-consistent calculations were performed, including all core electrons and a minimal basis set of augmented spherical waves (SW's), for the valence electrons containing 5s-, 5p-, and 4d-like functions for Mo, and 4s-, 4p-, and 3d-like functions for Ni. The calculated DOS was used for the computation of x-ray emission spectra in which the hole lifetime smooths the details of the DOS distribution. Therefore the self-consistent iteration was carried out with only 65 **k** points uniformly distributed in an irreducible part of the Brillouin zone (IBZ) which is equivalent to 343 points in the whole BZ. In Fig. 2 we show the local partial DOS of the $L1_2$ and orthorhombic structures for the Ni_3Mo alloy.

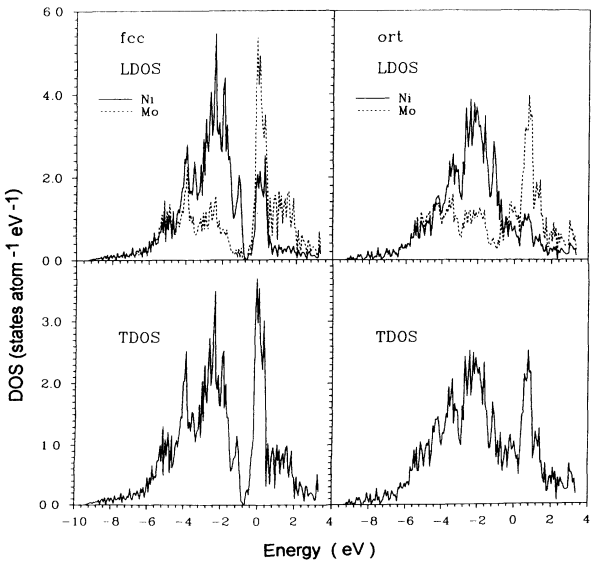

FIG. 2. The LDOS and TDOS calculated by making use of the LSW method for $L1_2$ and orthorhombic structures of the Ni_3Mo alloy.

C. Linear-muffin-tin-orbital method

The linear-muffin-tin-orbital (LMTO) method[20] was used to calculate the electronic band structure for elemental Ni and for the Ni_3Mo alloy under the assumption of an $L1_2$ type of order, and taking into account valence electrons of all symmetries. The exchange and correlation interactions were treated within the local-density approximation using the Barth-Hedin parametrization. Relativistic effects, except for spin-orbit coupling, were included in these calculations. We treated the outermost s, p, d, and f electrons as the valence states, while the charge density of the remaining electrons was kept fixed (the frozen-core approximation). In the self-consistent procedure, the diagonalization of the LMTO Hamiltonian was performed only at 35 **k** points in an irreducible part of the Brillouin zone. The loss of accuracy in this computation does not appear to affect the agreement between calculated and measured spectra, as discussed in Sec. IV (Fig. 6). The $s+d$-LDOS of Ni and TDOS for the $L1_2$ structure calculated by the tetrahedron method[17] are shown in Fig. 3(a).

All calculations provided a similar shape for DOS distribution, except for the lack of the s states in the TB model, and some changes in the intensity of some details

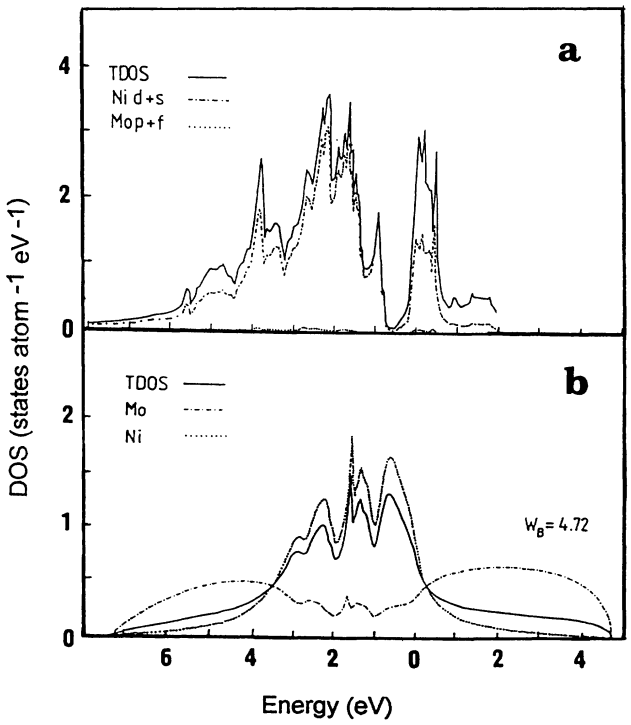

FIG. 3. (a) The LDOS and TDOS calculated by the LMTO method for the $L1_2$ structure of the Ni_3Mo alloy. (b) The LDOS and TDOS for random Ni_3Mo alloys calculated by making use of the CPA approximation for parameters $W_B=4.72$.

of the DOS structure which are too fine to be probed by XES.

D. Coherent-potential approximation

Considering the random fcc structure of the Ni_3Mo alloy, we assumed two limiting cases: (i) the $L1_2$ type of unit cell, and (ii) no preference for the Mo- or Ni-atom positions in the fcc unit cell. To calculate the d-LDOS and total TDOS in the second case, the coherent-potential approximation (CPA) (Ref. 21) was applied to the tight-binding model, in which the transfer integral as well as the atomic levels depends on the atomic species occupying the sites of the lattice.[22]

Velicky, Kirkpatrick, and Ehrenreich[23] have proved that the CPA is the best possible approximation within the so-called single-site approximation. The main concept of this approximation is based on defining a certain effective ordered system with corresponding effective potential functions which can be located at each site in the alloy and used to solve the Schrödinger equation. The best choice for the unknown effective coherent potential is then obtained by satisfying certain constraints. This model was used in calculations of the Ni_3Mo random-alloy electronic structure. The dimensionless parameter w_B describing the transfer integrals between atomic sites [proportional to $dd\sigma$ (Mo-Mo)/ $dd\sigma$(Ni-Ni)] (Ref. 23) was chosen to be equal to 4.72.[24] The separation between atomic levels was determined to satisfy the charge neutrality condition at each atomic site. In order to determine the Fermi energy, we assumed that the number of d electrons of Ni and Mo atoms is equal to 9.08 and 5.07 per atom, respectively.[23]

The results of the calculations are presented in Fig. 3(b). Comparing the DOS for disordered and ordered alloys, one can note the broadening of the band and smoothing of many details. The pronounced antibonding Mo d states located in ordered structure between 0 and 2 eV (up to three states per atom per eV) in disordered alloys are flatter (0.7 state per atoms per eV) and extend up to 5 eV. In the Ni bonding states, the maximum near the Fermi level disappears, and all states are shifted in the direction of zero energy. The disorder reduces the localization of the states.

IV. RESULTS AND DISCUSSION

The measured emission spectra of Ni in a Ni-Mo alloy are broader than for elemental Ni.[3] This effect is in disagreement with the theory of alloys.[25–27] The increase of Ni-Ni distances is expected to result in a stronger localization of the d-like states of Ni atoms, thus leading to the narrowing of the valence band. The broadening of the Ni spectra from alloys compared with elemental Ni spectra have also been observed earlier in Ni-Fe alloys.[28] Our considerations may help in understanding the above effect.

The results of Ni DOS calculations were the basis for the estimation of the shape of L_α Ni spectra. According to the dipole selection rule, the assumption is made that the transition of the d- and s-like symmetry valence electrons to the hole at the $2p_{3/2}$ level creates the basic $L_{\alpha 1,2}$ emission line. The spectra were calculated within the one-electron model. The lifetime width of the hole in the $2p_{3/2}$ core level and the final-state lifetime was approximated by the Lorentzian function with the energy-dependent full width at half maximum (FWHM) equal to $0.8 + 0.1 \times E$ (eV).[29] The instrumental function was estimated to be the Gaussian function with the FWHM equal to 0.5 eV.

These two phenomena broaden the LDOS distribution during the creation of x-ray valence emission spectra. The LDOS distribution was thus convoluted with the above-mentioned broadening functions. Additionally, the intensity distribution at the high-energy side of the experimental L_α spectra can be influenced by the self-absorption[30] and the satellite.[31] The intensity in the satellite line is derived from the multiple vacancy states, set up by radiationless Auger transitions from L_1 and L_2 initial states. The only way to avoid this satellite is to keep the energy of primary radiation below the energy of excitation of the $2p_{1/2}$ (L_2) level, which was not possible in our experimental arrangement. Nevertheless, in many cases, the satellite is sufficiently suppressed by self-absorption, and these two effects appeared to balance in our case. The self-absorption process depends on the geometry of spectra excitation. This geometry was optimized during the experiment to provide the largest intensity of the recorded spectra, and later was kept the same for all samples. Only the low-energy edge of the experimental spectra is completely free from additional effects. The calculated spectra were not corrected for these two effects.

The elemental Ni DOS and experimental and calculated Ni L_α spectra are presented in Fig. 4 for all methods of calculation. The intensities of the calculated and experimental spectra were normalized at the maximum. Spectra were matched to have the best agreement, and the position of zero energy in the experimental spectrum was selected at the same point as for the calculated spectra. The exact estimation of the Fermi-level position in experimental x-ray emission spectra is not a trivial task.[32] Usually x-ray-absorption spectra are helpful in estimating this position.[33] In our case, we concentrated on the overall shape of spectra for which the precise position of the Fermi level is not so important. Our results are similar to these presented, e.g., by Szmulowicz and Pease.[34] The spectra calculated for elemental Ni are about 1.2 eV broader than the width of the experimental spectrum, and this difference does not depend on the method of calculation used and similar discrepancies were observed in Ni photoelectron spectra.[4] Correlation effects are responsible for this discrepancy. These effects were accounted for by Kleinman,[35] and experimentally estimated by Starnberg and Nilsson.[36] This problem is documented in the literature, and therefore we concentrated on the question of the degree to which correlation effects influenced the Ni spectra from the alloy.

Comparisons of the experimental L_α spectrum for the random Ni_3Mo alloy, with spectra calculated on the basis of the CPA d-LDOS, are presented in Fig. 5(a). The calculated spectrum (full line) is about 0.5 eV broader at the

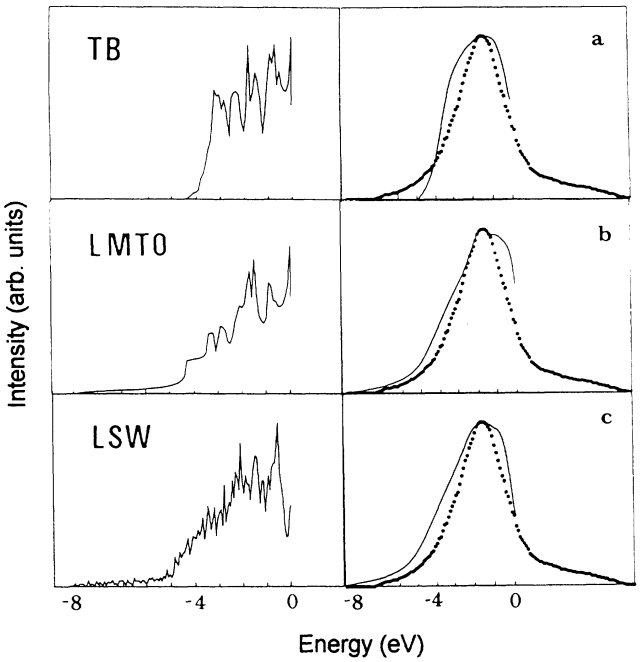

FIG. 4. The LDOS of Ni (left-hand panel); the experimental L_α spectrum of elemental Ni (dotted line); and results of the Ni spectrum calculation (solid line) on the basis of d-LDOS from (a) the TB method and Ni $d+s$-LDOS from (b) LMTO and (c) LSW methods (right-hand panel).

top than the experimental spectrum (dotted line). In the experimental spectrum we do not observe such a large delocalization of the states caused by disorder as appears in the CPA calculation. The presence of short-range order in the random Ni_3Mo alloy may be the explanation for the observed difference between calculated and experimental spectra.

To use methods applicable to ordered systems, an assumption of the $L1_2$ structure was made. The L_α spectra calculated on the basis of the d-LDOS, resulting from the tight-binding d-band model, and on the basis of the $d+s$-LDOS resulting from LMTO and LSW methods, are compared with the experimental spectrum of random alloy in Figs. 5(b), 5(c), and 5(d), respectively. The spectral calculated on the basis of the d-LDOS in the TB model show the correct width, but the low-energy side is not described properly. The lack of the s-LDOS in these calculations is the reason for this discrepancy. The best agreement was obtained when the spectrum was calculated on the basis of the $d+s$-LDOS, resulting from the LMTO and LSW methods under an assumption of $L1_2$ ordering in the so-called random alloy. The increase in accuracy of calculations from 35 **k** points in LMTO to 64 **k** points in an irreducible part of the Brillouin zone in LSW does not influence the overall agreement of calculated and experimental spectra. The natural width of the core level smooths the details in the LDOS structure. However, the width of the calculated spectrum at the top is still somewhat smaller than the width of the experimental spectrum. This can be correlated with the deviation from assumed order in the occupancy of atomic positions in the random alloy, which was not taken into account by the LMTO and LSW methods. The above observation indicates that even in the so-called random alloys some local order in positions of neighboring atoms exists. The general structure of the valence band is influenced mostly by the first-neighbor atoms. All models of DOS calculations provide the correct basic shape of the L_α spectrum. Computed spectra differ only in details of the intensity distribution. The correlation effects are not important in the case of the Ni spectra recorded for the alloy. The addition of a second element (Mo) leads to an increase of the distance between Ni atoms (2.49 Å in elemental Ni, and 2.567 Å in the Ni_3Mo alloy), which results in the reduction of many-body effects. The observed broadening of the Ni spectra from alloys, as compared with the spectrum of elemental Ni, is due to the reduction of the correlation effects.

The agreement of the high-energy side of calculated and measured spectra is also satisfactory. Good agreement of the high-energy side of spectra indicate that the geometry chosen for the excitation was correct, and that the self-absorption sufficiently suppressed the satellite intensity.

We now consider the influence of the unit-cell symme-

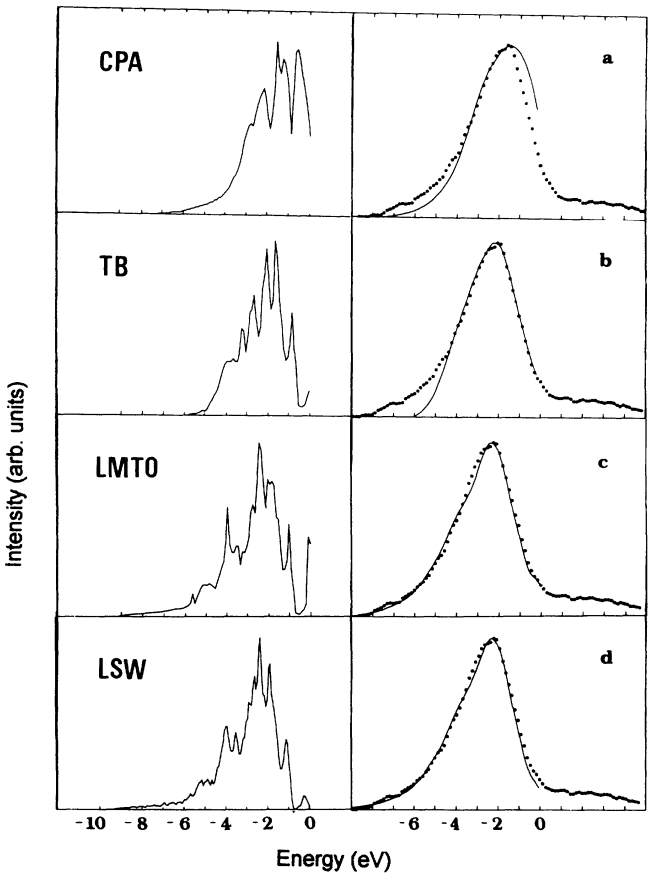

FIG. 5. The LDOS of Ni (left-hand panel); the experimental Ni L_α spectrum for random Ni_3Mo alloys (dotted line); and results of L_α spectra calculations (solid line) on the basis of the Ni d-LDOS from (a) CPA and (b) tight-binding (TB) methods and the Ni $d+s$-LDOS from (c) LMTO and (d) LSW methods (right-hand panel).

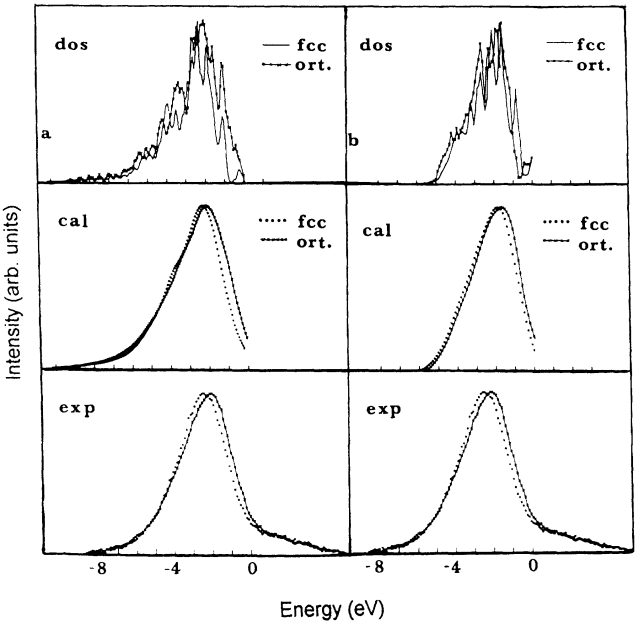

FIG. 6. (a) The results of LSW calculations of the $d+s$-LDOS for $L1_2$ (solid line) and orthorhombic structures (solid-crossed line) of Ni_3Mo alloys (upper panel); the Ni L_α spectra calculated on the basis of these DOS (in the middle), and the experimental Ni L_α spectra for random (dotted line) and ordered (solid-crossed line) orthorhombic Ni_3Mo alloys (lower panel). (b) The results of TB calculations of the d-LDOS for $L1_2$ (solid line) and orthorhombic structures (solid-crossed line) of Ni_3Mo alloys (upper panel); the Ni L_α spectra calculated on the basis of these DOS (in the middle), and the experimental Ni L_α spectra for random (dotted line) and ordered (solid-crossed line) orthorhombic Ni_3Mo alloys (lower panel).

try and thus the number and distances of Ni nearest-neighbor atoms on the magnitude of the correlation effects. The ordering of the Ni_3Mo alloy results in the formation of an orthorhombic structure with eight atoms in the unit cell (12 atoms in the fcc unit cell). The d-LDOS of Ni for the ordered alloy was calculated by the TB d-band model, and the $s+d$-LDOS by the LSW method. The Ni L_α spectra were calculated in a manner similar to that above. Both methods lead to spectra which are in agreement with the experiment (cf. Fig. 6). Comparing the fine structure of calculated and experimental spectra for $L1_2$ and orthorhombic crystal structures, one notices that the peak is broader and the intensity at the Fermi level is sharper for the orthorhombic structure than for the $L1_2$ structure. This indicates that the change in the number and distances of atoms in the unit cell around the emitting Ni atom leads to a redistribution of valence d-like electrons near the Fermi level. However, the rearrangement of atoms around an emitting Ni atom does not change the significance of correlation effects in the Ni-emission spectrum.

V. SUMMARY

We have presented studies of the LDOS for elemental Ni and Ni in random and ordered Ni_3Mo, using several methods of calculation, and a comparison of the results with experimental L_α-emission spectra of Ni. The observed broadening of Ni spectra from alloys, as compared with the spectrum of elemental Ni, is due to the reduction of correlation effects. The addition of a second element (Mo) leads to increased Ni-Ni distances, which results in the reduction of the magnitude of many-body effects. The CPA method was used to calculate the LDOS for random alloys under the assumption of statistical occupancy of the sites by Ni and Mo atoms in the fcc unit cell. The spectrum resulting from these calculations is too broad at the top, and the intensity at the low-energy side of the spectrum is underestimated. This indicates the presence of some short-range order in the alloy.

The TB, LMTO, and LSW methods were used to calculate the LDOS in the alloy, under the assumption of an $L1_2$ structure. The TB d-band model provides a spectrum with the proper width, but the intensity at the low-energy side is underestimated. This is a consequence of the lack of a delocalized s-LDOS in this model, and indicates the importance of the s states in the creation of L_α Ni spectra. The best agreement of the spectra was found for the LMTO and LSW methods.

The change in atomic order and distances in the unit cell around the emitting atom leads to a redistribution of the valence d-like electrons near the Fermi level. This is predicted correctly by the theoretical models, and is also observed in the L_α Ni-emission spectra. The change in the atomic order and distances in the unit cell around the emitting atom does not influence the significance of the correlation effects on L_α Ni-emission spectra.

ACKNOWLEDGMENT

The authors would like to thank Dr. W. Paszkowicz for the x-ray-diffraction measurements, and for a critical reading of the manuscript.

[1]See, e.g., *Soft X-Ray Band Spectra and Electronic Structure of Metals and Materials*, edited by D. J. Fabian (Academic, London, 1968).

[2]C. Bonnelle, in *Soft X-Ray Band Spectra and Electronic Structure of Metals and Materials* (Ref. 1), p. 163.

[3]K. Ławniczak-Jabłońska, J. A. Leiro, and L. I. Nikolaev, X-Ray Spectrometry **17**, 223 (1988), and references therein.

[4]L. C. Davis, J. Appl. Phys. **59**, R25 (1985), and references therein.

[5]S. Satio and P. B. Beck, Trans. Metall. Soc. AIME, **215**, 938 (1959).

[6]L. Dargiel-Sulir and H. Jankowski, Thin Solid Films **141**, 129 (1986).

[7]M. R. Khan, C. S. L. Chun, G. P. Felcher, M. Grimsditch, A.

Kueny, C. M. Falco, and I. K. Schuller, Phys. Rev. B **27**, 7186 (1983).

[8]G. Cocco, S. Enzo, N. Barrett, and K. J. Roberts, in *Proceedings of the Second European Conference on Progress in X-ray Synchrotron Radiation Research, Roma 1989,* edited by A. Balerna, E. Bernieri, and S. Mobilio (Italian Physical Society, Bologna, 1990), p. 693.

[9]A. Balzarotti, N. Motta, A. Kisiel, M. Zimnal-Starnawska, M. T. Czyżyk, and M. Podgorny, Phys. Rev. B **31**, 7526 (1985).

[10]J. B. Boyce and J. C. Mikkelsen, Jr., J. Cryst. Growth **98**, 37 (1989).

[11]M. T. Czyżyk, K. Ławniczak-Jabłońska, and S. Mobilio, Phys. Rev. B **45**, 1581 (1992).

[12]J. C. Slater and G. F. Koster, Phys. Rev. **94**, 1498 (1954).

[13]J. Inoue and M. Shimizu, J. Phys. F **15**, 1511 (1985); **17**, 2067 (1987).

[14]R. E. W. Casselton and W. Hume-Rothery, J. Less-Common Metals **7**, 212 (1964).

[15]D. G. Pettifor, J. Phys. F **7**, 613 (1977).

[16]O. K. Andersen and O. Jepsen, Physica B **91**, 317 (1977).

[17]J. Rath and A. J. Freeman, Phys. Rev. B **11**, 2109 (1975).

[18]K. Ławniczak-Jabłońska and M. Heinonen, J. Phys. F **18**, 2451 (1988).

[19]H. van Leuken, A. Lodder, M. T. Czyżyk, F. Springelkamp, and R. A. de Groot, Phys. Rev. B **41**, 5613 (1990).

[20]H. L. Skriver, *The LMTO Method* (Springer, Berlin, 1984).

[21]P. Soven, Phys. Rev. **156**, 809 (1967); Phys. Rev. B **2**, 4715 (1970).

[22]H. Shiba, Prog. Theor. Phys. **46**, 77 (1971).

[23]B. Velicky, S. Kirkpatrick, and H. Ehrenreich, Phys. Rev. **175**, 747 (1968).

[24]K. Ławniczak-Jabłońska, J. Inoue, and K. Tohyama, in *Proceedings of the Second International Seminar on X-Ray and Electron Spectroscopy, Madralin 1989,* edited by J. Auleytner and K. Ławniczak-Jabłónska (Polish Academy of Sciences, Warszawa, 1989), p. 99.

[25]R. C. Young, Rep., Prog. Phys. **40**, 75 (1977).

[26]V. L. Moruzzi, A. R. Williams, J. F. Janak, and C. Sofes, Phys. Rev. B **9**, 3316 (1974).

[27]J. S. Faulkner and G. M. Stocks, Phys. Rev. B **23**, 5628 (1981).

[28]K. Ławniczak-Jabłońska and J. Auleytner, J. Phys. F **12**, 2279 (1982).

[29]J. E. Müller, O. Jepsen, and J. W. Wilkins, Solid State Commun. **42**, 365 (1982).

[30]C. Bonnelle, Ann. Phys. (Paris) **1**, 439 (1966).

[31]R. Liefeld, in *Soft X-Ray Band Structure and Electronic Structure of Metals and Materials* (Ref. 1), p. 133.

[32]J. R. Cuthill, A. J. McAlister, A. M. L. Williams, and R. E. Watson, Phys. Rev. **164**, 1006 (1967).

[33]K. S. Song, J. Phys. (Paris) Colloq. **28**, C3-43 (1967).

[34]F. Szmulowicz and D. M. Pease, Phys. Rev. B **17**, 3341 (1978).

[35]L. Kleinman, Phys. Rev. B **19**, 1295 (1979).

[36]H. I. Starnberg and P. O. Nilsson, J. Phys. F **18**, L247 (1988).